NUMERICAL BENCHMARK OF STRONGLY TO LOOSELY COUPLED ASSEMBLIES USING THE TRANSIENT FISSION MATRIX METHOD

K. Routsonis[1], P. Blaise[1], and J. Tommasi[2]

[1]DEN/CAD/DER/SPESI, CEA Cadarache,
13108 Saint Paul-Lez-Durance, France

[2]DEN/CAD/DER/SPRC, CEA Cadarache,
13108 Saint Paul-Lez-Durance, France

kornilios.routsonis@cea.fr, *patrick.blaise@cea.fr*, *jean.tommasi@cea.fr*

ABSTRACT

Advances in computational methods have given rise to the study and simulation of different aspects of reactor behavior. As such, topics associated with high computational costs become feasible candidates for further investigation and one of them is reactor space-time kinetics (STK). Until recently, STK simulation and point kinetics approximation were limited to deterministic codes, with Monte Carlo codes being too costly to start with. However, recent developments in this area have allowed the use of certain methods in stochastic codes. One such technique is based on the Transient Fission Matrix (TFM) model, a hybrid method that uses a system response obtained through Monte Carlo and stored in fission and time matrices as input for deterministic calculations. The result enables a view of the STK in terms of neutron propagation probability and propagation time across the system. The TFM method was applied to a simple coupled core configuration to generate a numerical benchmark. The Serpent 2 Monte Carlo code was used for the stochastic part of the calculation. The configuration consists of two fuel assemblies placed in a light water tank, with a water blade of varying width between them. TFM, flux and fission results were obtained for varying water blade widths, ranging between 0 cm and 20 cm. The data is then used to analyze the behavior of the system, as well as the effects of the coupling between the two assemblies. As the assemblies move further apart, the system slowly transitions from two tightly coupled assemblies that essentially form a single core, to two almost independent cores. This study enables to produce a benchmark for future calculations and predefine an innovative way of designing high dominant ratio configurations, required for tackling Monte Carlo residual problems. An actual experimental program could be led in ad hoc zero power reactor (ZPR), such as the KUCA reactor of Kyoto University.

KEYWORDS: TFM, kinetics, Monte Carlo, Serpent, matrix

1. INTRODUCTION

Until recently, most widely used stochastic transport codes lacked native support for reactor kinetics calculations. With initial versions of such modules becoming available, research into the field or reactor space-time kinetics will likely experience an increase in the near future. Today, such research is fragmented and limited, incorporating local, in-house solutions, tested in various different geometries. The numerical benchmark presented in this paper aims to bring relevant research together, by offering a common and

easily reproducible configuration, both in codes and experiments, to test existing and future calculation methods and models. The Transient Fission Matrix [1-4] application here and its results present a benchmark for future comparisons. A system of coupled assemblies was used and analyzed at different stages of coupling, as the behavior of coupled fissile systems represents a good case study. As part of the benchmark, the full set of fission-to-fission probability TFM matrices is available for prompt and delayed neutrons, alongside the average neutron fission-to-fission time matrices for the prompt-to-prompt case, as well as flux results. For the sake of brevity, this work presents a part of the TFM results for the geometry analyzed in this project. The system utilizes PWR-style fuel assemblies, with reactor grade UOX fuel (UOX – UOX system) and a second version is currently being studied, where one assembly will use MOX fuel (UOX – MOX), in order to investigate the effect between two differently reactive fuels. The effect of control rod insertion is also being studied. The results are obtained with the Serpent 2 Monte Carlo code [5].

2. CALCULATION SETUP AND RELEVANT THEORY

2.1. The Coupled Assembly System

The geometry is kept simple on purpose, consisting of a light water tank and two parallel rows of PWR assemblies placed inside, separated by an adaptive water blade between them. Black boundary conditions were used for the x and z axes and periodic boundary conditions for the y-axis. The assemblies are free to move along the x-axis of the geometry, essentially changing the width of the water blade. Below, Fig. 1 shows an x-y view of the UOX – UOX case.

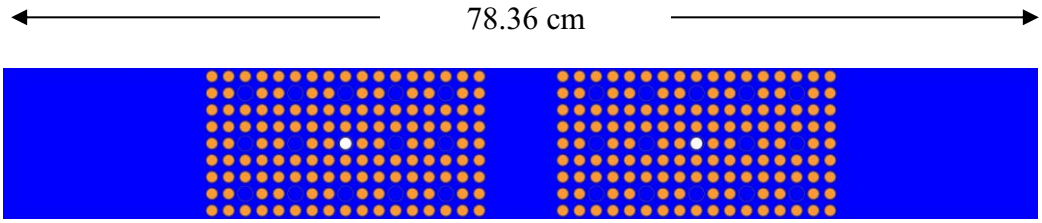

Figure 1. X-Y view of the UOX – UOX geometry, with a water blade of 5.04 cm

For TFM and detector calculations, the geometry is meshed in a way that the mesh structure is always a multiple of the number of pin-cells (62 along the x-axis). This allows results to be easily expressed in both SI units and in relation to the lattice pitch.

2.2. Coupled Core Systems and Multipoint Kinetics

The following approach to multipoint reactor kinetics was developed by K. Kobayashi [6,7]. He showed that, for a system of coupled reactors, the static and kinetic nodal equations can be respectively derived from the static and time-dependent multigroup equations.

Consider a multiple reactor system V and its boundary S with the boundary condition

$$\psi_g(\boldsymbol{r},\boldsymbol{\Omega}) = 0 \quad , \quad \text{for } \boldsymbol{\Omega}\cdot\boldsymbol{n} < 0 \ \text{ at } \ \boldsymbol{r} \in S \tag{1}$$

where ψ_g denotes the total angular flux of the g[th] group, for direction $\boldsymbol{\Omega}$ and $\boldsymbol{n}$ is the outward unit vector normal to surface S. An unperturbed steady-state system with a criticality factor k can be described by

$$A\psi_g(\boldsymbol{r},\boldsymbol{\Omega}) = \frac{1}{k} B\psi_g(\boldsymbol{r},\boldsymbol{\Omega}) \tag{2}$$

$$A\psi_g(\boldsymbol{r},\boldsymbol{\Omega}) = \left(\boldsymbol{\Omega}\boldsymbol{\nabla} + \Sigma_{t,g}\right)\psi_g(\boldsymbol{r},\boldsymbol{\Omega}) - \sum_{g'}\int_{4\pi} d\boldsymbol{\Omega}'\,\Sigma_s(g,\boldsymbol{\Omega}\leftarrow g',\boldsymbol{\Omega}')\psi_{g'}(\boldsymbol{r},\boldsymbol{\Omega}') \quad (3)$$

$$B\psi_g(\boldsymbol{r},\boldsymbol{\Omega}) = \frac{\chi_g}{4\pi}\sum_{g'}\nu\Sigma_{f,g'}(\boldsymbol{r},\boldsymbol{\Omega})\int_{4\pi} d\boldsymbol{\Omega}\,\psi_{g'}(\boldsymbol{r},\boldsymbol{\Omega}) = \frac{\chi_g}{4\pi}F\psi_g(\boldsymbol{r},\boldsymbol{\Omega}) \quad (4)$$

$$F\psi_g(\boldsymbol{r},\boldsymbol{\Omega}) = \sum_{g'}\nu\Sigma_{f,g'}(\boldsymbol{r})\int_{4\pi} d\boldsymbol{\Omega}\,\psi_{g'}(\boldsymbol{r},\boldsymbol{\Omega}) \quad (5)$$

where $\Sigma_{t,g}$, $\nu\Sigma_{f,g}$ and χ_g are the total cross section, average neutron production through fission and average fission neutron spectrum for group g respectively. $\Sigma_s(g,\boldsymbol{\Omega}\leftarrow g',\boldsymbol{\Omega}')$ denotes the scattering cross section from group g' and direction $\boldsymbol{\Omega}'$ to group g and direction $\boldsymbol{\Omega}$. A Green's function is defined through

$$A^{\dagger}G(\boldsymbol{r},\boldsymbol{\Omega},g;\boldsymbol{r}',g') = \delta(\boldsymbol{r}-\boldsymbol{r}')\delta_{gg'}\ ,\ \text{for}\ \ \boldsymbol{\Omega}\cdot\boldsymbol{n} > 0\ \text{at}\ \boldsymbol{r}\in S \quad (6)$$

Integrating over the system V and the solid angle and summing the energy groups yields

$$\int_{4\pi} d\boldsymbol{\Omega}\,\psi_{g'}(\boldsymbol{r}',\boldsymbol{\Omega}) = \frac{1}{4\pi k}\int_V d\boldsymbol{r}\int_{4\pi} d\boldsymbol{\Omega}\sum_g G(\boldsymbol{r},\boldsymbol{\Omega},g;\boldsymbol{r}',g')\chi_g S(\boldsymbol{r}) \quad (7)$$

Where $S(\boldsymbol{r})$ is the number of neutrons produced per unit volume and unit time and is defined by

$$S(\boldsymbol{r}) = \sum_{g'}\nu\Sigma_{f,g'}(\boldsymbol{r})\int_{4\pi} d\boldsymbol{\Omega}\,\psi_{g'}(\boldsymbol{r},\boldsymbol{\Omega}) = F\psi_g(\boldsymbol{r},\boldsymbol{\Omega}) \quad (8)$$

Taking $\int_{4\pi} d\boldsymbol{\Omega}\,\psi_{g'}(\boldsymbol{r}',\boldsymbol{\Omega})$, multiplying by $\nu\Sigma_{f,g'}(\boldsymbol{r}')$, summing over all energies and interchanging g and g' and $\boldsymbol{r}$ and $\boldsymbol{r}'$**,** yields

$$S(\boldsymbol{r}) = \frac{1}{4\pi k}\sum_g \nu\Sigma_{f,g}(\boldsymbol{r})\int_V d\boldsymbol{r}'\int_{4\pi} d\boldsymbol{\Omega}'\sum_{g'} G(\boldsymbol{r}',\boldsymbol{\Omega}',g';\boldsymbol{r},g)\chi_{g'}S(\boldsymbol{r}') \quad (9)$$

This is an integral equation for the fission source $S(\boldsymbol{r})$ and can be solved if the corresponding Green's function is known. For a region in the system V, denoted as V_i, that has a non zero fission cross section, the following importance function is introduced

$$G_i(\boldsymbol{r},\boldsymbol{\Omega},g) = \int_{V_i} d\boldsymbol{r}'\sum_{g'}\nu\Sigma_{f,g'}(\boldsymbol{r}')G(\boldsymbol{r},\boldsymbol{\Omega}',g;\boldsymbol{r}',g') \quad (10)$$

and

$$A^{\dagger}G_i(\boldsymbol{r},\boldsymbol{\Omega},g) = \nu\Sigma_{f,g}(\boldsymbol{r})\delta_i(\boldsymbol{r}),\ \ \delta_i(\boldsymbol{r}) = \begin{cases}1, & r\in V_i\\ 0, & r\notin V_i\end{cases} \quad (11)$$

G_i expresses the expected number of fission neutrons born in V_i by a neutron born at position $\boldsymbol{r}$, with direction $\boldsymbol{\Omega}$ and its energy within group g. The solution of G_i can be obtained by solving the adjoint multigroup equation with the fixed term $\nu\Sigma_{f,g}(\boldsymbol{r})$ in the region V_i. Integrating over V_i yields Eq. (13) below,

$$\begin{aligned} S_i &= \frac{1}{4\pi k}\int_V d\boldsymbol{r}'\int_{4\pi} d\boldsymbol{\Omega}'\sum_{g'} G(\boldsymbol{r}',\boldsymbol{\Omega}',g';\boldsymbol{r},g)\chi_{g'}S(\boldsymbol{r}') = \\ &= \int_{V_i} d\boldsymbol{r}S(\boldsymbol{r}) = \int_{V_i} d\boldsymbol{r}\sum_g \nu\Sigma_{f,g}(\boldsymbol{r})\int_{4\pi} d\boldsymbol{\Omega}\,\psi_g(\boldsymbol{r},\boldsymbol{\Omega}) \end{aligned} \quad (12)$$

The coupling coefficient between two regions V_i and V_j is given by

$$k_{ij} = \frac{\frac{1}{4\pi}\int_{V_j} d\boldsymbol{r}'\int_{4\pi} d\boldsymbol{\Omega}'\sum_{g'} G(\boldsymbol{r}',\boldsymbol{\Omega}',g')\chi_{g'}S(\boldsymbol{r}')}{\int_{V_j} d\boldsymbol{r}'S(\boldsymbol{r}')} \quad (13)$$

and expresses the expected number of fission neutrons produced in V_i by a fission neutron born in V_j.

2.3. The Transient Fission Matrix model

The Transient Fission Matrix (TFM) model [1-4], allows for the spatial kinetic modeling of a nuclear system by pre-calculating the time dependent transport characteristics. The information contained in a fission matrix $\underline{G}$ is the probability that a neutron born in volume j (or V_j) produces a new fission neutron in a volume i (or V_i), where V_i and are volumes of a discretized geometry (propagation probability). The information is presented in four matrices, according to the neutron emission spectrum χ and the multiplicity ν, differentiating between prompt and delayed cases. Delayed neutron information is condensed and presented in one delayed group. There is a clear connection between the $\underline{G}_{\chi_p \nu_p}$, $\underline{G}_{\chi_p \nu_d}$, $\underline{G}_{\chi_d \nu_p}$ and $\underline{G}_{\chi_d \nu_d}$ matrices produced by the TFM model and the aforementioned coupling coefficients. In principle, summing the different neutron propagation probabilities over all neutron spectra and lifetimes for one generation, should wield region-wise coupling coefficients that agree with the ones calculated from Eq. 13 or are reasonably close.

The temporal aspect, a requirement to deal in kinetics with fission matrices, is covered by obtaining the average neutron fission-to-fission time. The available output is the average neutron fission-to-fission time (propagation time) from j to i, which is stored in the $\underline{T}_{\chi_p \nu_p}$ matrix. The TFM approach was initially developed for fast reactors but it has been successfully demonstrated that it produces accurate results for thermal reactor behavior as well. The process does introduce a geometrical bias in the calculation [2] of the multiplication factor due to the discretization of the fission matrix, which decreases as the number of meshes goes up. In this work, the TFM model runs on an in-house modified version of the Serpent 2 Monte Carlo code.

3. TFM RESULTS FOR THE UOX – UOX CASE

The calculation results are presented below, for the UOX – UOX case. They are comprised of the TFM probability and fission-to-fission time matrices, as well as flux and fission rate results. Fig. 2 shows the $\underline{G}_{\chi_p \nu_p}$ matrices for a water blade width of 0, 2.52, 5.04 and 20.16 cm (0, 2, 4 and 16 pitch lengths, respectively).

The initial case at 0 cm blade width gives a certain picture; the two assemblies are operating as a single, continuous system. Fission probability is the highest near the point of origin of a fission neutron, as the system is thermal and the neutron's migration length is small. The two assemblies contribute greatly to each other's fission events near the boundary and it is clear that the two systems are tightly coupled.

It is apparent that as the water blade width between the two assemblies increases, the system transitions from a single fissile geometry to two independent ones, all coupling between the two assemblies having been reduced to practically zero. The two assemblies, initially contributing significantly to each other's fission rates near the boundary, are at the end operating like two separate thermal systems, as the reflection effect of the moderator starts becoming more and more prominent. Due to the reflection, propagation probability increases locally, especially for the $i \cong j$ cases at the assembly boundaries, since any neutrons with emission angles towards the moderator either do not contribute to fissions at all (and so the information is lost) or are reflected and, now thermalized, induce fissions at the lattice boundary. At the 20 cm case, there is no discernible difference between the inner and outer boundaries of the two assemblies, both sides being almost fully reflected. The above are further corroborated by the rest of the $\underline{G}$ matrices as well, as shown in Fig. 3

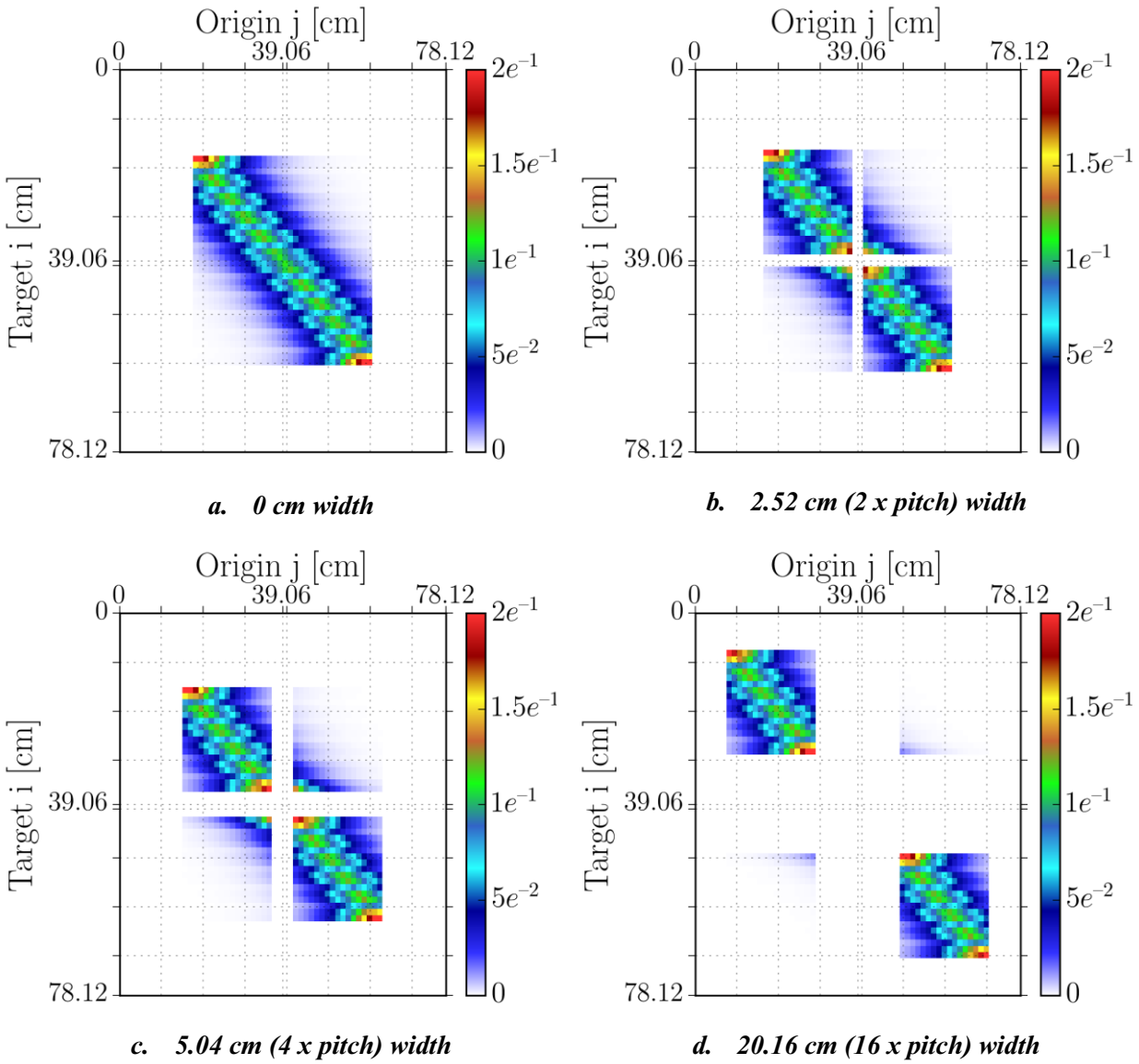

a. 0 cm width

b. 2.52 cm (2 x pitch) width

c. 5.04 cm (4 x pitch) width

d. 20.16 cm (16 x pitch) width

Figure 2. $\underline{G}_{\chi_p \nu_p}$ matrices for the UOX – UOX geometry, for different water blade widths. The color scale expresses the propagation probability.

Additionally, the $\underline{T}_{\chi_p \nu_p}$ matrices, shown in Fig. 4, clearly show the gradual transition to two decoupled and reflected assemblies. Fig. 3b already highlights that behavior and it only becomes more prominent as the separation increases. As the two assemblies are separated, the average fission-to-fission time becomes greater in the now reflected inner boundaries, since most neutrons that contribute to fissions undergo full thermalization beforehand.

Fig. 5 shows that due to the decoupling between the assemblies because of the water blade, the insertion of negative reactivity in the right assembly has little effect on the left's prompt neutron propagation probability. The probability of contributed fission does not change in a significant manner. There is still an influx of thermal neutrons from the left to the right assembly, as shown in Fig. 6, but the flux changes by

an order of magnitude and the probability for prompt-to-prompt local events is greatly diminished in the right assembly. This points to the high degree of decoupling already present at this stage.

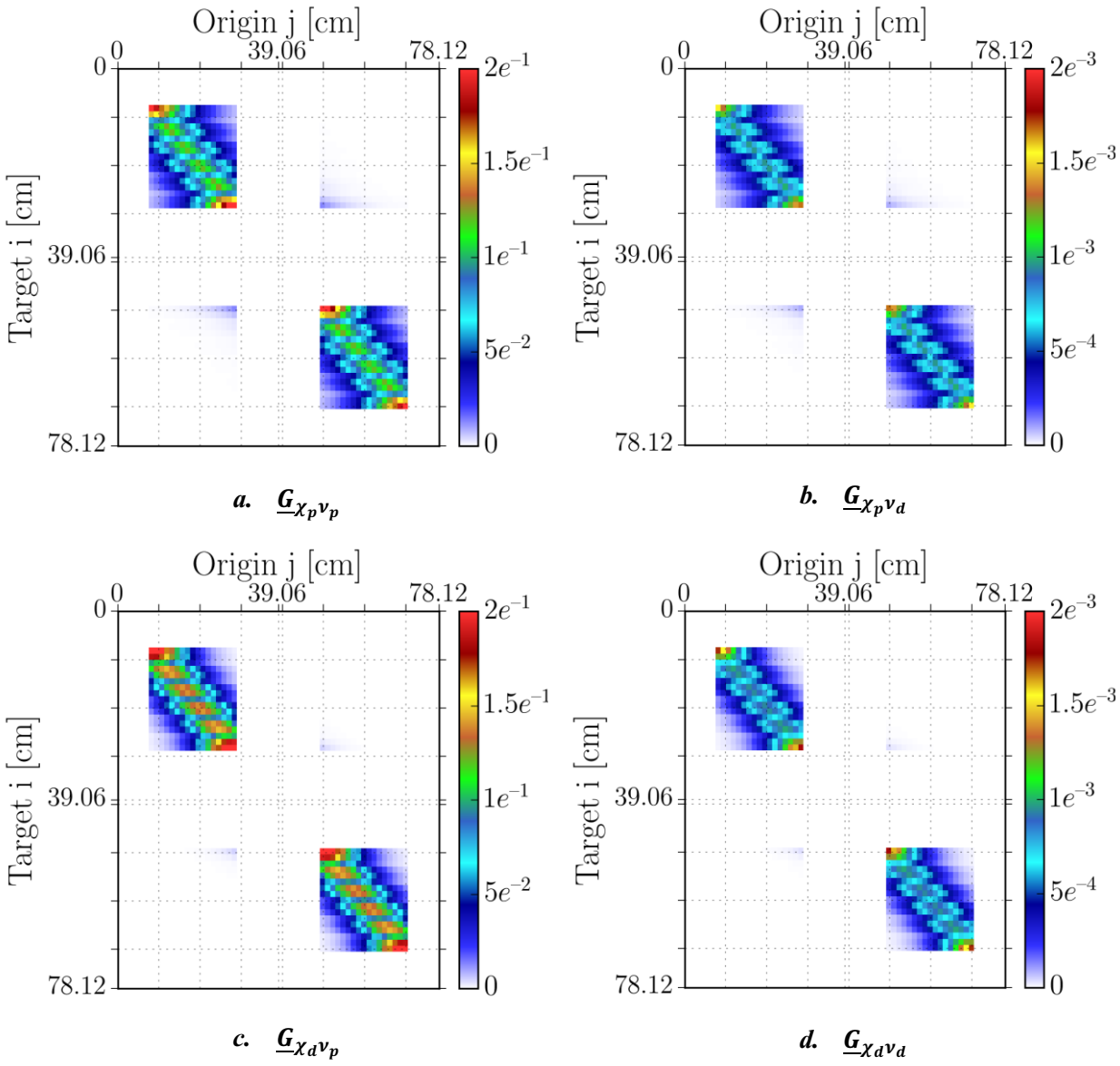

Figure 3. $\underline{G}$ matrices for the UOX – UOX geometry, for a 20.16 cm *(16 x pitch)* water blade width. The color scale expresses the propagation probability.

Lastly, Fig. 6 gives the thermal flux shape across the traverse of the geometry, in 248 bins (4 bins per pin-cell), including the case of control rod insertion, with B_4C control rods inserted in the guide tubes of the rightmost assembly. The thing to note here is the flux shape difference between the "5.04 cm" and "5.04 cm CR" cases. With control rods inserted, the right assembly acts as a very weak neutron source and so the left's flux and reaction rate is not affected by it in any significant way, its flux shape going from sloped to almost flat and symmetrical. At the same time, the right assembly's flux shape is greatly affected by incoming flux from the left, while its fission rate is greatly diminished and mostly flat (not pictured).

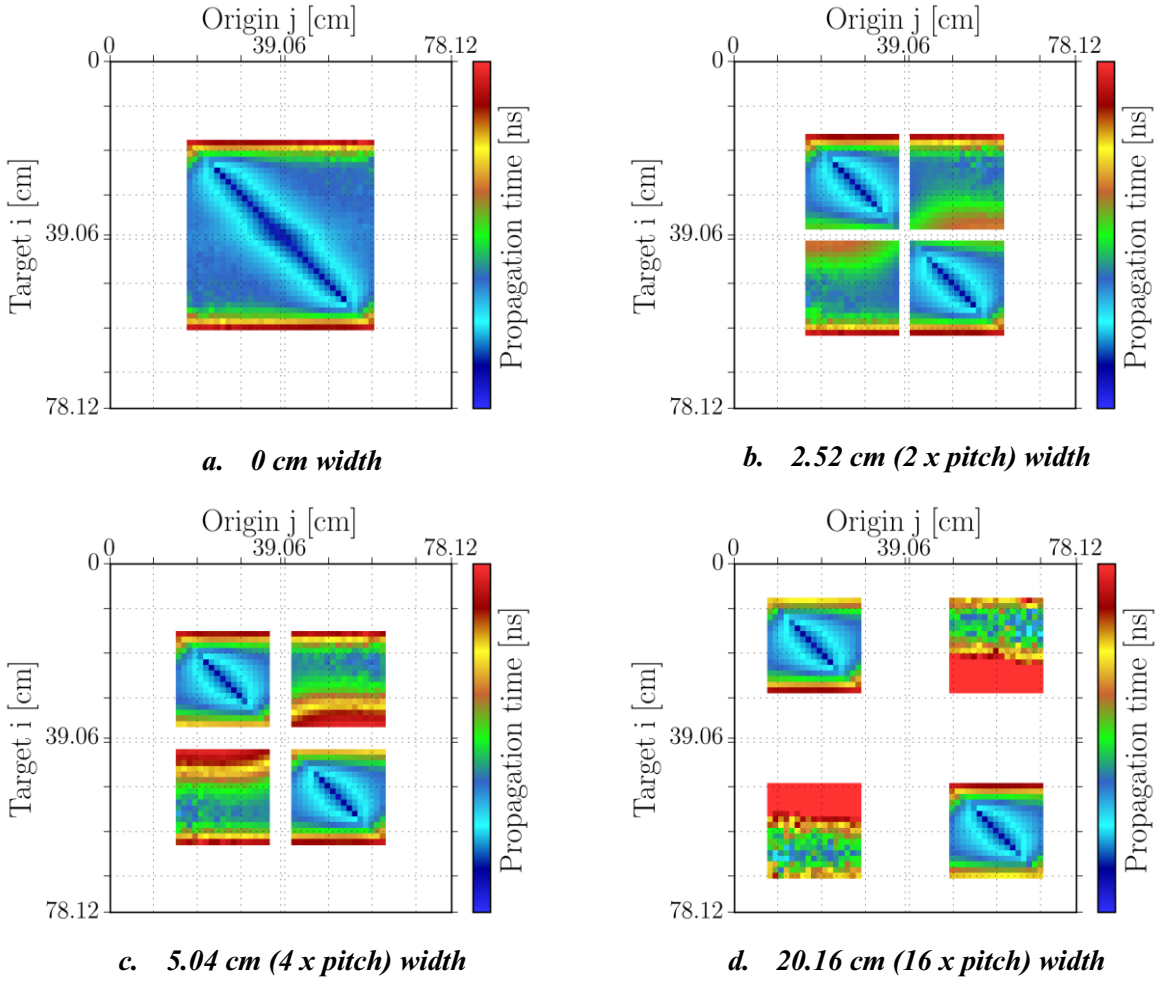

a. 0 cm width ***b. 2.52 cm (2 x pitch) width***

c. 5.04 cm (4 x pitch) width ***d. 20.16 cm (16 x pitch) width***

Figure 4. $\underline{T}_{\chi_p \nu_p}$ matrices for the UOX – UOX geometry, for different water blade widths. The color scale expresses the propagation time and goes from 20 µs to 80 µs.

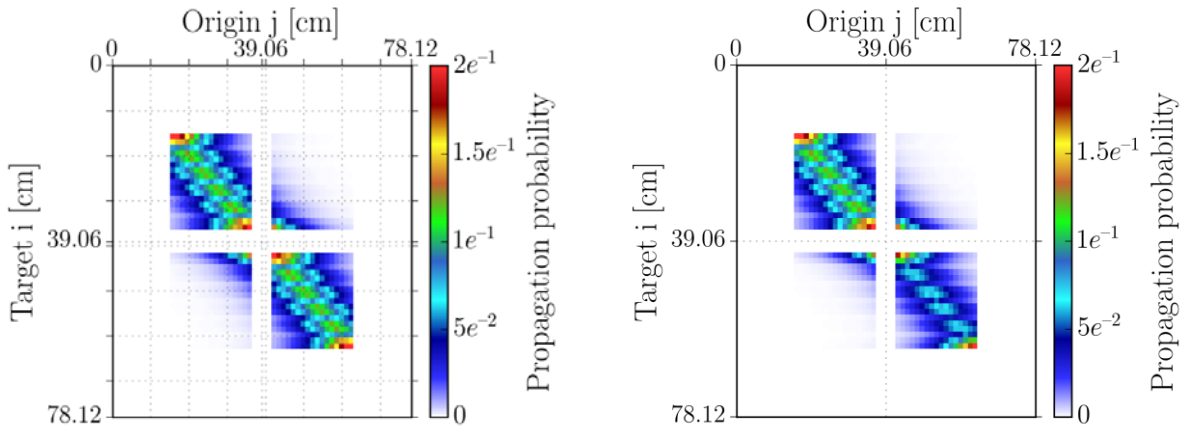

a. Clean configuration ***b. Control rods inserted to the right***

Figure 5. $\underline{G}_{\chi_p \nu_p}$ matrices for the a water blade width of 5.04cm, showing the effect of rod insertion.

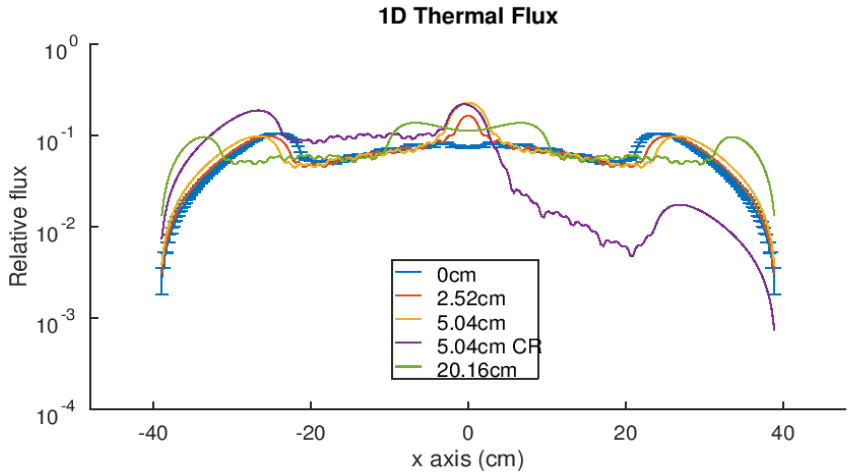

Figure 6. 1D thermal flux, including the result of control rod insertion (5.04cm CR).

4. CONCLUSIONS

A detailed numerical benchmark based on an UOX – UOX assembly coupled system was developed in order to help in the comprehensive study of reactor kinetics effects by offering a common ground for the application and testing of calculation schemes. A large number of relevant results were generated and are presented in this paper, including flux calculations, transient fission matrices and importance plots, at various stages of coupling. The test case also includes the effects of control rod insertion. The results available in this paper show the coupled system response as the assemblies move apart and transition from a single fissile geometry to two essentially independent, reflected assemblies. The method used to analyze the geometry runs on an in-house modified version of the Serpent 2 Monte Carlo code. The work was extended to a UOX – MOX system, in order to point out different coupling amplitudes due to less reactive fuels and different delayed neutron fractions, as well as compared to multipoint kinetics calculations. It will be presented in a forthcoming publication.

REFERENCES

1. Laureau, L. Buiron, B. Fontaine, "Local correlated sampling Monte Carlo calculations in the TFM neutronics approach for spatial and point kinetics applications", *EPJ Nuclear Sci. Technol*., **3**(16) (2017).
2. A. Laureau, L. Buiron, B. Fontaine, "Towards spatial kinetics in a low void effect sodium fast reactor: core analysis and validation of the TFM neutronic approach", *EPJ Nuclear Sci. Technol.,* **3**(17) (2017).
3. A. Laureau, L. Buiron, B. Fontaine, V. Pascal, "Fission Matrix Interpolation for the TFM Approach Based on a Local Correlated Sampling Technique for Fast Spectrum Heterogeneous Reactors", *Proc. Int.Conf. M&C 2017*, Jeju, Korea, April 16-20 (2017).
4. P. Blaise, A. Laureau, P. Ros, P. Leconte, K. Routsonis, "Transient Fission Matrix approach for assessing complex kinetics behavior in the ZEPHYR ZPR coupled core configurations", *Ann. Nucl. Energy,* **128** pp. 390-397 (2019).
5. J. Leppänen, M. Pusa, T. Viitanen, V. Valtavirta, T. Kaltiaisenaho, "The Serpent Monte Carlo code: status, development and applications in 2013", *Ann. Nucl. Energy,* **82** (2015).
6. K. Kobayashi "A relation of the Coupling coefficient to the eigenvalue separation in the coupled reactors theory", *Ann. Nucl. Energy,* **25**, pp. 198-201 (1998).
7. K. Kobayashi "Rigorous Derivation of Multi-Point Reactor Kinetics Equations with Explicit Dependence on Perturbation", *Journal of Nuclear Science and Technology,* **29**(2), pp. 110-120 (1992).